Proceedings World Geothermal Congress 2000
Kyushu - Tohoku, Japan, May 28 - June 10, 2000

FRACTURE CHARACTERIZATION USING SINGLE-HOLE EM DATA

Soon Jee Seol[1], Yoonho Song[1], and Ki Ha Lee[2]
[1]Korea Institute of Geology, Mining and Materials, 30 Kajung-Dong, Yusung-Gu, Taejon 305-350, Korea
[2]Ernest Orlando Lawrence Berkeley National Laboratory, 1 Cyclotron Road, Berkeley, CA 94720, U.S.A.

Key words: fracture, single-hole, EM, inversion

ABSTRACT

A simple method of mapping fractures in terms of a few fracture parameters is presented in this paper. Frequency-domain 3-component electromagnetic (EM) fields measured in a single-hole configuration are used for the analysis. In actual producing fields the fracture geometry and surrounding medium can be very complicated. For precise imaging of such a fractured medium, it will take a full-fledged 3-D EM inversion that will involve a great deal of computing resources. Success of such an effort may not be guaranteed because of the lack of data inherent to the single-hole survey method.

For simplicity, it is assumed that the medium is a uniform whole space, and the parameters to be inverted are the background conductivity, the distance, conductance and dip angle of a single fracture of large extent. In obtaining these parameters, a combination of simulated annealing (SA) and nonlinear least-squares (NLSQ) methods have been used. The SA is an excellent searching algorithm leading to the general vicinity of the global minimum, thereby providing reasonably good initial guess for the NLSQ. Detailed fine-tuning of inversion parameters can then be accomplished through NLSQ with an accelerated convergence. The approach has been very successful in determining fracture parameters. Data used for the tests are synthetic, generated by a 1-D medium with a thin layer and by a thin sheet in a whole space.

The proposed method is useful for analyzing models of simple geometry. But since the approach is simple and computationally efficient, it can be used real-time in producing fields for fast evaluation of the reservoir in which fluid flow is controlled by fractures. Additionally, results obtained in this manner may be useful in preparing an initial model for a more rigorous 3-D EM inversion at a later time.

1. INTRODUCTION

Mapping fractures and other permeable zones in a producing geothermal field is important because these features are the conduits of geothermal fluids. Precise description of these structures can guide drilling and optimize long-term reservoir management. An important geophysical parameter that can be used to infer the existence of fractures and help in mapping them is electrical conductivity. Electrical conductivity is a function of porosity, saturation, the type and state of the fluid, and hydraulic permeability of the rock. The petroleum and geothermal industries have used resistivity well logs to map variations in pore fluid, to distinguish rock types, and to determine well completion intervals. Although inductive resistivity logging has long been an important tool for sensing variations in reservoir properties, the depth of investigation is limited to the immediate vicinity of the well bore. These conventional well log data do not contain information about the directional property of the anomalous feature because of the scalar nature of the measurements.

Recently developed borehole EM tools provide more complete borehole EM data with improved quality. The device termed GEO-BILT (Geothermal Borehole Induction Logging) under development by Electromagnetic Instruments Inc. (EMI) is one new tool designed for single-hole use. The new tools are equipped with a multi-frequency transmitter and multi-offset receiver modules, each of which consists of 3-component sensors for directional information.

In conjunction with the new tool development, we have been investigating imaging algorithms for mapping fractures in a single-hole configuration. A three-step fracture imaging scheme using single-hole EM data in the high frequency range between several hundreds of kilo-hertz and several tens of mega-hertz already exists (Seol et al., 1998). As the next step of this study, we have developed an inversion algorithm for characterizing a fracture using the conventional low frequency range in a simple formation. We assume the fracture is an inclined inductive thin layer in a homogeneous whole space. For the proposed method to be successful, we first need to use two horizontal components to determine the strike of the sheet. In the presence of a vertical magnetic dipole, the strike of the fracture is in the direction of null horizontal magnetic field. Once this is completed then we are ready to move to the next step of mapping the fracture using the approach described in this paper.

2. MODEL RESPONSE CALCULATION

In our preliminary study of fracture detection, we used the EM1D (Pellerin et al., 1995) code to simulate EM responses of a thin conductor of infinite extent. The code is known to provide accurate EM responses of a layered earth when excited by an arbitrary dipole source. The fracture is simulated with a thin layer with thickness of 0.1 m and the strike is set to *y*-axis. Thus the y component of horizontal magnetic field is null for the vertical magnetic source. The arbitrary dip is realized through rotation of coordinates. After rotation, the *x* and *z* coordinates are interchanged to follow the conventional cartesian coordinate system with positive downward *z*. Figure 1 shows the schematic diagram of coordinate transform. A vertical magnetic dipole (M_z) of unit moment was used as a source. In the transformed primed coordinate system, both horizontal ($M_{x'}$) and vertical ($M_{z'}$) magnetic sources are necessary to calculate magnetic fields due to vertical magnetic source in the field (unprimed) coordinate system. Magnetic fields in the field coordinate are obtained through vector sum of horizontal and vertical magnetic fields due to $M_{x'}$ and $M_{z'}$, respectively. These procedures are described as follows.

The rotation and interchange of coordinates are given by

$$\begin{pmatrix} x' \\ z' \end{pmatrix} = \begin{pmatrix} 0 & -1 \\ 1 & 0 \end{pmatrix} \begin{pmatrix} \cos\theta & \sin\theta \\ -\sin\theta & \cos\theta \end{pmatrix} \begin{pmatrix} x \\ z \end{pmatrix} \quad (1)$$

The horizontal and vertical magnetic fields in the primed coordinate system are obtained by a vector sum of those due to $M_{x'}$ and $M_{z'}$ sources, i.e.,

$$H_{x'} = H_{x'x'} + H_{x'z'}, \quad (2)$$

$$H_{z'} = H_{z'x'} + H_{z'z'}. \quad (3)$$

Here H_{ij} means the *i*-th component of magnetic field due to the *j*-directed magnetic dipole source.
Finally, the horizontal and vertical magnetic fields in the field coordinate are given by

$$H_x = H_{x'}\sin\theta + H_{z'}\cos\theta, \quad (4)$$

$$H_z = -H_{x'}\cos\theta + H_{z'}\sin\theta. \quad (5)$$

3. INVERSION EXPERIMENTS

In characterizing a fracture using single-hole EM data, the inversion problem consists of evaluating the conductivity of the background medium (c_b), the conductivity (c_f) and inclination angle (a_f) of the fracture, and the normal distance from the coordinate origin to the fracture (d_f). To examine some major features of the inverse problem, we chose the model shown in Figure 2. The *x*-direction is set to be perpendicular to the strike of the fracture and its thickness is fixed at 0.1 m. The background medium and the fracture have conductivities of 0.01 S/m and 4 S/m, respectively. The normal distance from the coordinate origin to the fracture is 10 m. Since the dip angle of the fracture is assigned at 70°, the inclination angle is 20°. A vertical magnetic dipole source is used and three receivers are located at 2, 4, and 6 m below the source. The magnetic fields at these three receivers are used for the inversion procedure. The other parameters are indicated on the illustration. In all calculation, magnetic permeability is assumed to be that of free space value.

3.1 Fracture responses

The horizontal and vertical magnetic fields are obtained for the model shown in Figure 2 at the first receiver along the *z*-axis. Frequencies used are 30 kHz and 300 kHz. Figure 3 shows the real (left) and imaginary (right) components of the total horizontal and vertical magnetic fields. As the source is moved down, the distance from the source to the fracture is reduced, until finally the borehole intersects the fracture at the depth of 29.2 m. The responses show significant dependence on the distance between source and fracture in both H_x and H_z fields. In other words, we have to use data at sufficiently close source and receivers from a fracture for successful inversion. The criteria may be analyzed by considering both the skin depth and fracture conductivity.

3.2 Error contours

To investigate the characteristics of our inverse problem, we examine global properties of the prediction error in terms of RMS. The RMS error is defined as

$$RMS = \sqrt{\frac{1}{N}\sum_{i=1}^{4}\sum_{j=1}^{nr\times nf}\frac{\left[f_{i,j}(\mathbf{m}^{est}) - f_{i,j}(\mathbf{m}^{t})\right]^2}{f_{i,j}(\mathbf{m}^{est})}}, \quad (6)$$

where $f(\mathbf{m}^{est})$ is the magnetic fields calculated for estimated model $\mathbf{m}^{est}$, $f(\mathbf{m}^{t})$ the magnetic fields calculated for the true model $\mathbf{m}^{t}$, subscript i the real and the imaginary parts of two components (H_x and H_z), *nr* the number of receiver positions, *nf* the number of frequencies, and $N = 4\times nr\times nf$ the number of data.

Figure 4 shows error contours as a function of two inversion parameters when the other two parameters are held fixed at their true values. For all parameter sets, except for the combination of c_b and c_f, two parameters are in different physical units. The contours show maximum and/or local minimum near global minimum except for Figure 4 (a). In particular, the RMS is very sensitive to the changes in d_f when an estimated value is smaller than the true one in all contours (Figure 4 (b), (d) and (f)). Since decreasing d_f has similar effects on the magnetic fields to increasing a_f at a given receiver position, the contours of d_f and a_f (Figure 4 (f)) demonstrate another minimum when d_f has smaller value than the true one, while a_f is near 70°. Data from multiple-offset receivers may reduce this difficulty in the inversion process. All these analyses manifest that the inversion result would have strong dependence on the initial guess.

3.3 NLSQ and SA

For estimating the four parameters, we use a nonlinear damped least-squares method (NLSQ), in which the observation equation was solved directly using the Householder transformation (Press et al., 1992). The Frechet derivatives are calculated through the numerical differentiation of magnetic fields with respect to each parameter. Table 1 shows the inversion results of NLSQ for the infinite fracture model as shown in Figure 2. All four parameters are exactly resolved after 7 iterations. In this case we assigned a good initial guess based on the error contours. When we assigned other initial guesses as shown Table 2, we failed to get the solutions using NLSQ.

To overcome the strong dependence of NLSQ on the initial guess, we apply a simulated annealing method (SA) incorporating the modified downhill simplex method (Press et al., 1992; Kim et al., 1997). The SA technique has attracted significant attention as being suitable for optimization problems where a desired global minimum is hidden among many local minima (Sen and Stoffa, 1995). Table 2 shows inversion results of SA for the infinite fracture model after 300 iterations. As expected, all four parameters are fully resolved.

3.4 Combining NLSQ with SA

SA has little dependence on initial guess, but it takes a lot of computing time to find the solution. Even though the down-hill simplex method used in SA accelerates the parameters approach near to the true values, they converge very slowly to

the exact values. Therefore, we have designed a combined inversion scheme of NLSQ and SA. The first step of inversion is to determine an initial guess for NLSQ using SA. The second step is to apply NLSQ inversion starting from this initial guess. Table 3 shows the inversion results using the combined approach for the infinite fracture model. SA produces a good initial guess for NLSQ after several iterations, and all four parameters are exactly resolved by NLSQ after 4 iterations.

3.5 Fracture with finite dimension

We have also tested our inversion scheme for the fracture with finite dimension. This finite fracture is simulated using the thin sheet integral equation EM modeling code WSHEET which is a whole space version of HFSHEET (Song and Lee, 1998). The dimension of the fracture is 100 m $\times$ 100 m and the other parameters are set to be the same as the infinite fracture case (Figure 2) used in the previous test. The inversion result using the combined scheme is shown in Table 4. NLSQ starting from an initial guess provided by SA gives successful results after 5 iterations. It suggests that this inversion scheme can be applied to map realistic finite fractures when the fracture dimension is large enough.

4. CONCLUSIONS

Mapping fractures of simple geometry is, in principle, possible using data obtained from single-hole survey configuration. In this study we have only used one fixed source and three receiver positions, at each of which we assumed we have 3-component magnetic fields.

Generally, data can be collected for multiple source positions with multiple offset receivers. This is good because data from the source close to the dipping sheet will provide more sensitive information about the fracture. Combinations of data from sources at varying distance to the fracture will broaden the spatial coverage and help improve inversion results.

ACKNOWLEDGMENTS

This work was supported by the Assistant Secretary for Energy Efficiency and Renewable Energy, Geothermal Division of the U.S. Department of Energy under Contract No. DE-AC03-76SF00098. The first author was also funded by Korea Science and Engineering Foundation (KOSEF). The authors would like to acknowledge Prof. Hee Joon Kim for his valuable suggestions towards improving the quality of this work.

REFERENCES

Kim, H.J., Song, Y.H., and Lee, K.H. (1997), High-frequency electromagnetic inversion for a dispersive layered earth, *J. Geomag. Geoelectr.*, Vol. 49, pp. 1439-1450.

Pellerin, L., Labson, V.F., and Pfeifer, M.C. (1995). VETEM-A very early time electromagnetic system-, *Proceeding of the Symposium on the Application of Geophysics to Engineering and Environmental Problems (SAGEEP)*, pp. 725-731.

Press, W.H., Teukolsky, S.A., Vetterling, W.T., and Flannery, B.P. (1992), *Numerical Recipes in Fortran, 2nd ed.*, Cambridge Univ. Press.

Sen, M. and P.L. Stoffa (1995), *Global Optimization Methods in Geophysical Inversion*, Elsevier, 281pp.

Seol, S.J., Song, Y., Kim, H.J., and Lee, K.H. (1998), Fracture imaging using high-frequency single-hole EM data, *Proceedings of the 4th SEGJ International Symposium*, pp. 245-252.

Song, Y., and Lee, K.H. (1998), A wide-band integral equation solution for EM scattering by thin sheets, *68th Ann. Internat. Mtg., Soc. Expl. Geophys., Expanded Abstracts*, pp.436-439.

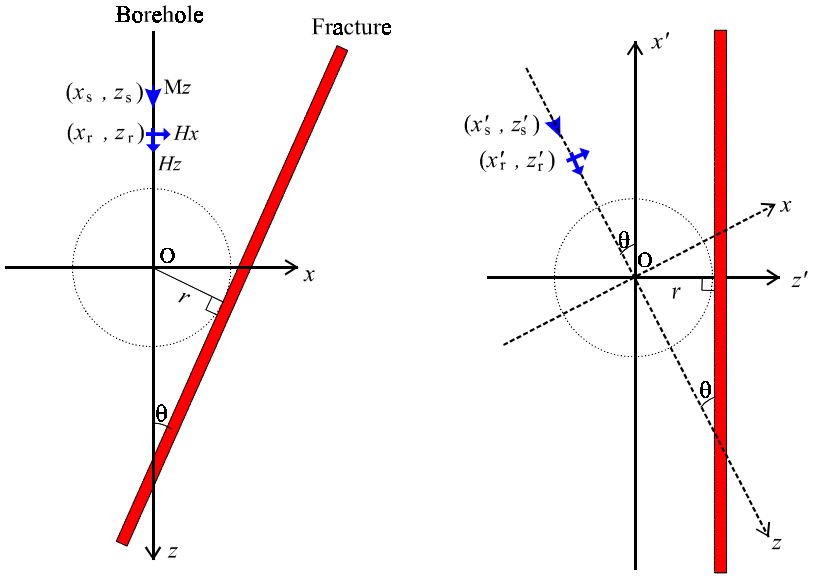

Figure 1. Schematic presentation of coordinate transform. The unprimed cartesian coordinate is transformed to the primed coordinate for simulating a dipping fracture with infinite dimension using EM1D.

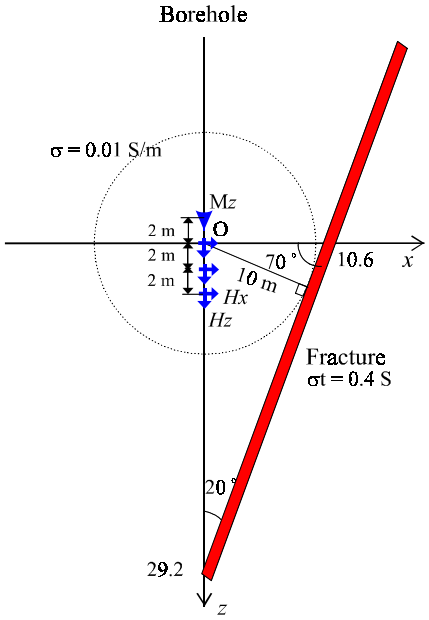

Figure 2. Model and survey configuration used in inversion. The fracture has 0.1 m thickness and infinite extent.

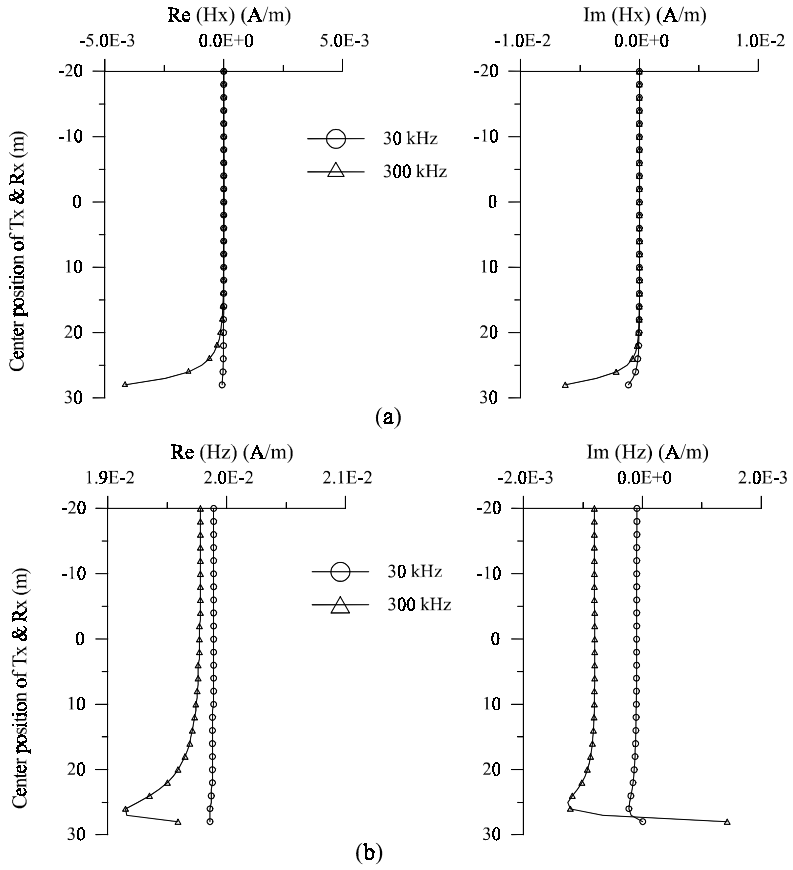

Figure 3. Total *Hx* (a) and *Hz* (b) fields for the model shown in Figure 2 at the first receiver. Data were obtained by vertical profiling along the *z*-axis and plotted at each center position of source and receiver.

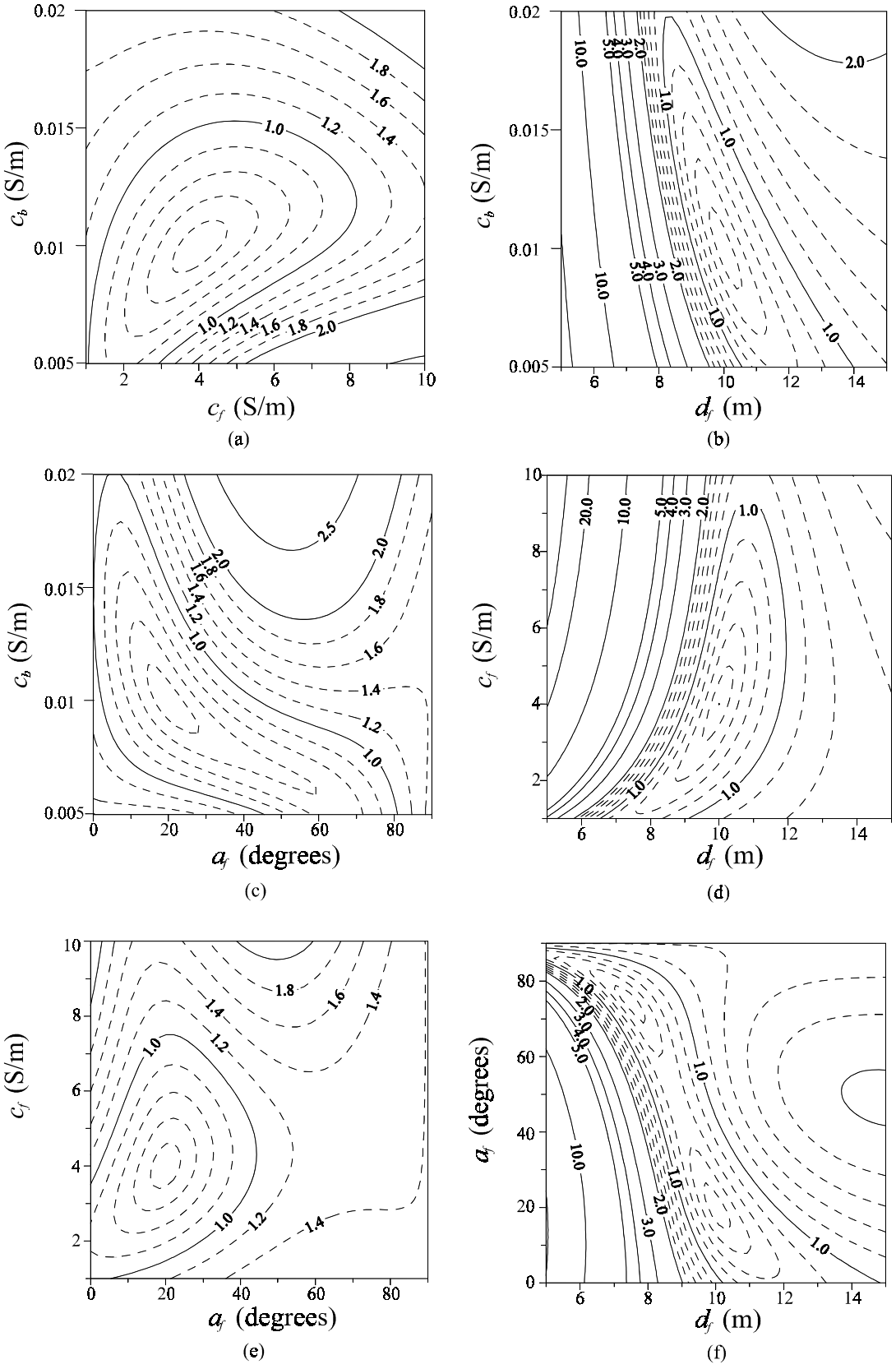

Figure 4. Error contours as a function of two inversion parameters when the other two parameters are fixed to true values. The true values for four parameters are c_b = 0.01 S/m, c_f = 4 S/m, d_f = 10 m, and a_f = 20°.

Table 1. NLSQ inversion results after 7 iterations for the infinite fracture model

Parameter	True	Initial	Inversion
c_b (S/m)	0.01	0.005	0.01 ± 0.0 %
c_f (S/m)	4	10	4.00 ± 0.0 %
d_f (m)	10	5	10.00 ± 0.0 %
a_f (degree)	20	5	20.00 ± 0.0 %
RMS error	0.1194×10^{-3}	97.64	0.1829×10^{-3}

Table 2. SA inversion results after 300 iterations for the infinite fracture model

Parameter	True	Initial	Inversion
c_b (S/m)	0.01	0.02	0.9905×10^{-2}
c_f (S/m)	4	10	4.013
d_f (m)	10	20	10.02
a_f (degree)	20	45	20.07
RMS error	0.1194×10^{-3}	0.9523	0.5405×10^{-2}

Table 3. NLSQ inversion using the initial guess determined by SA for the infinite fracture model. The initial guess for NLSQ is obtained by SA after 10 iterations and the inversion results are obtained by NLSQ after 4 iterations.

Parameter	True	Initial for SA	Initial for NLSQ	Inversion
c_b (S/m)	0.01	0.02	0.5772×10^{-2}	0.01 ± 0.0 %
c_f (S/m)	4	10	6.661	4.00 ± 0.0 %
d_f (m)	10	20	11.85	10.00 ± 0.0 %
a_f (degree)	20	45	20.51	20.00 ± 0.0 %
RMS error	0.1194×10^{-3}	0.9523	0.1022	0.1179×10^{-3}

Table 4. NLSQ inversion using the initial guess determined by SA for the finite fracture model of 100 m × 100 m size. The initial guess for NLSQ was obtained by SA after 10 iterations and the inversion results are obtained by NLSQ after 5 iterations.

Parameter	True	Initial for SA	Initial for NLSQ	Inversion
c_b (S/m)	0.01	0.02	0.693×10^{-2}	0.01 ± 0.3 %
c_f (S/m)	4	10	6.97	3.925 ± 0.3 %
d_f (m)	10	20	11.6	10.01 ± 0.1 %
a_f (degree)	20	45	16.7	20.69 ± 0.2 %
RMS error	0.7526×10^{-1}	0.9513	0.2408	0.5955×10^{-2}